Hindawi Publishing Corporation
Journal of Engineering
Volume 2013, Article ID 391083, 8 pages
http://dx.doi.org/10.1155/2013/391083

Research Article

Synthesis and Microwave Absorbing Properties of Cu-Doped Nickel Zinc Ferrite/$Pb(Zr_{0.52}Ti_{0.48})O_3$ Nanocomposites

Avinandan Mandal, Debasis Ghosh, Asish Malas, Parthajit Pal, and Chapal Kumar Das

Materials Science Centre, Indian Institute of Technology Kharagpur, Kharagpur 721302, West Bengal, India

Correspondence should be addressed to Chapal Kumar Das; chapal12@yahoo.co.in

Received 31 August 2012; Revised 7 December 2012; Accepted 9 December 2012

Academic Editor: Guangming Xie

Nanocomposites based on Cu-doped nickel zinc ferrite and lead zirconium titanate exhibited significant microwave absorbing properties in the X-band (8.2–12.4 GHz) region. Coprecipitation and homogeneous precipitation methods were utilized to synthesize Cu-doped nickel zinc ferrite ($Cu_{0.2}Ni_{0.4}Zn_{0.4}Fe_2O_4$) and lead zirconium titanate ($Pb(Zr_{0.52}Ti_{0.48})O_3$) nanoparticles, respectively. To develop nanocomposites, dispersion of these nanoparticles into epoxy resin (LY665) polymeric matrix was carried out by using mechanical stirrer. Phase analyses of the nanoparticles were done by X-ray diffraction (XRD). Moreover, morphological characterization was done by scanning electron microscopy (SEM) and transmission electron microscopy (TEM). Energy dispersive X-ray spectroscopy (EDS) confirmed the chemical constituents present in the nanocomposites. Complex relative permittivity ($\varepsilon_r = \varepsilon' - j\varepsilon''$) and complex relative permeability ($\mu_r = \mu' - j\mu''$) values of the nanocomposites were measured in different microwave frequencies in the X-band (8.2–12.4 GHz) region by employing vector network analyzer (model PNA E8364B), and return loss (dB) values were calculated to identify the microwave absorbing performance of the present nanocomposites. Brilliant microwave absorbing properties have been achieved by the nanocomposites with the minimum return loss of −49.53 dB at 8.44 GHz when sample thickness was 3 mm. For the present nanocomposites, mainly dielectric loss was responsible for loss mechanism.

1. Introduction

In recent decades, low-cost, light weight microwave absorbing materials in the gigahertz frequency range have attracted in both commercial and military purposes. The microwave absorbing materials are employed to reduce the electromagnetic reflection from metal plates such as air crafts, tanks, ships, and electronic equipments [1–4]. These classes of materials are very interesting because of their unique absorbing properties of microwave energy and used in different applications like reduction of radar (Radio Detection and Ranging) cross-sectional area, television image interference of high rise building, microwave dark-room, shielding of electromagnetic interference [5–7], and so forth. In the present research work, we focused on the development of radar absorbing materials mainly for military purposes. To absorb microwave energy, there are several materials that are acting as radar absorbers including dielectric and magnetic materials [8–10]. Extensive literature survey has been carried out to prepare radar absorbing materials with a high dielectric and magnetic loss [11–14]. Based on our knowledge, we have taken $Cu_{0.2}Ni_{0.4}Zn_{0.4}Fe_2O_4$ (Cu-NZF) nanoparticles as ferromagnetic material and $Pb(Zr_{0.52}Ti_{0.48})O_3$(PZT) nanoparticles as ferroelectric material. Both the particles have been mixed in different compositions, that is, 3 : 1, 1 : 1, and 1 : 3 ratios by using ball mill for 1 hour. Epoxy resin, polyurethane, poly chloroprene, EPDM, and so forth can be utilized as polymeric matrix. Epoxy resins have unique properties like excellent adhesive, chemical and heat resistance, excellent mechanical properties, and very good electrical insulating properties. The composite materials were developed by distributing these mixture particulates into epoxy resin matrix. To investigate possible mechanism of microwave power absorption, we have measured complex relative permittivity ($\varepsilon_r = \varepsilon' - j\varepsilon''$), and permeability ($\mu_r = \mu' - j\mu''$) values of the nanocomposites by employing vector network analyzer (model PNA E8364B). According to transmission line theory, the return loss (dB)

Table 1: Compositions and maximum absorbing properties of the developed nanocomposites.

Sample code	Composition (30% filler)	minimum return loss (−dB)	Frequency (GHz)	Matching thickness (mm)
Sample-1	Cu-NZF	29.85	8.79	3
Sample-2	Cu-NZF/PZT (3 : 1)	43.82	8.95	3
Sample-3	Cu-NZF/PZT (1 : 1)	49.53	8.44	3
Sample-4	Cu-NZF/PZT (1 : 3)	46.36	9.04	2.75
Sample-5	PZT	37.46	8.37	3

values were evaluated from the permittivity and permeability values at a given frequency and a certain absorber thickness by using the expression [15] $R_L = -20\log_{10}[|(z_{\text{in}} - z_0)/(z_{\text{in}} + z_0)|]$, where $z_{\text{in}} = z_0\sqrt{(\mu_r/\varepsilon_r)}\tanh[(-j2\pi/c)(\sqrt{\varepsilon_r\mu_r})fd]$ is the characteristic input impedance of absorber, Z_0 is the free space impedance, f is the frequency of electromagnetic wave, d is the thickness of absorber, and c is the velocity of light. To get superior microwave absorbing properties, the characteristic input impedance of an absorber should be equal to the impedance of free space with a certain thickness of absorber, that is, $Z_{\text{in}} = Z_0$. The better results come when impedance match occurred. Characteristic input impedance depends on permittivity, permeability, operating frequency, and thickness of the absorbers. At a particular operating frequency, permittivity and permeability values of an absorber are the same but at different sample thickness, the absorber exhibited different absorbing properties. At a particular thickness, the absorber showed maximum return loss; that is, impedance matching occurred at one particular sample thickness. It is a well-known fact that permeability values are less important at higher frequency in the GHz range due to Snoek's limit [16]. In case of the present absorbers, the microwave power absorption occurs mainly due to dielectric loss.

2. Experimental Section

2.1. Materials. Titanium tetrachloride ($TiCl_4$), Zirconium oxychloride ($ZrOCl_2{\cdot}8H_2O$), urea (CH_4N_2O), and nickel nitrate (Ni $(NO_3)_2$, $6H_2O$) of analytical reagent grade were purchased from Merck chemicals (India). Copper nitrate (Cu $(NO_3)_2{\cdot}6H_2O$), zinc nitrate (Zn $(NO_3)_2{\cdot}6H_2O$), ferric nitrate (Fe $(NO_3)_3{\cdot}9H_2O$), lead chloride ($PbCl_2$), and sodium hydroxide (NaOH) of analytical reagent grade were obtained from Loba Chemie (India). All the reagents have been used without further purification. Distilled water was used in all the experiments.

2.2. Preparation of $Cu_{0.2}Ni_{0.4}Zn_{0.4}Fe_2O_4$ Nanoparticles. Coprecipitation method has been applied for the synthesis of $Cu_{0.2}Ni_{0.4}Zn_{0.4}Fe_2O_4$ nanoparticles [17]. Stoichiometric amount of $Fe(NO_3)_3{\cdot}9H_2O$, $Co(NO_3)_2{\cdot}6H_2O$, $Zn(NO_3)_2{\cdot}6H_2O$, and $Ni(NO_3)_2{\cdot}6H_2O$ salt solutions was mixed thoroughly by using magnetic stirrer at 80°C followed by the addition of boiling NaOH solution (molar ratio of OH/Cu-NZF was taken 8) with continuous stirring for 60 minutes at 100°C to complete the reaction. The resulting suspension was washed with water and with acetone several times. After filtration, the precipitate was dried at 60°C and calcined for 2 hours at 600°C to promote formation of spinel phase.

2.3. Preparation of $Pb(Zr_{0.52}Ti_{0.48})O_3$ Nanoparticles. $Pb(Zr_{0.52}Ti_{0.48})O_3$ nanoparticles were prepared by homogeneous precipitation method [18]. Stoichiometric amounts of $ZrOCl_2{\cdot}8H_2O$, $PbCl_2$ were dissolved individually in distilled water. In ethanol $TiCl_4$ was poured slowly because a violent reaction occurs when water is added to $TiCl_4$ and the three chloride ion solutions were mixed in a glass beaker. Urea was used as precipitating agent for this reaction. After heating at 90°C for 1 hour, the clear reaction mixture turned to turbid solution and the heating was continued for further two hours. This precipitate was collected by filtration, dried, and finally calcined this powder at 750°C for 6 hours to promote the formation of perovskite phase of lead zirconium titanate.

2.4. Development of Microwave Test Plate. Epoxy resin (LY556) was used as polymeric matrix due to its superior mechanical properties, better adhesive property, and so forth. The prepared nanoparticles were dispersed in epoxy resin matrices at 80°C with the help of mechanical stirrer for 1 hour and cured at 75°C for 30 minutes by using ethylene-di-amine as a hardener. Filler concentration was kept as 30% in all the samples and thickness of the samples was 2.25–3 mm. Total five samples were fabricated in different compositions; Table 1 contains the compositions of the absorbers. Cu-substituted nickel zinc ferrite (Cu-NZF) was dispersed in epoxy resin matrix to develop Sample-1. Cu-substituted nickel zinc ferrite (Cu-NZF) and lead zirconium titanate (PZT) nanoparticles have been mixed at the ratios of 3 : 1, 1 : 1, and 1 : 3 by ball milling for one hour and then by dispersing these mixed powder particulates in polymeric matrices. Samples-2, -3, and -4 were prepared, respectively. Horizontal type common ball mill was utilized for mixing the nanoparticles and ball to powder weight ratio was taken as 10 : 1. Sample-2 contained 22.5% Cu-NZF, 7.5% PZT, Sample-3 had 15% of both fillers, and Sample-4 contained 7.5% Cu-NZF, 22.5% PZT. Lead zirconium titanate was spread into polymeric matrix to develop Sample-5. The samples were cut exactly as rectangular shapes of size (0.9×0.4) inch^2 to fit into X-band waveguide for microwave measurement.

3. Characterization

The phase analysis of the nanoparticles was investigated by X-ray diffraction (XRD), Rigaku X-ray Diffractometer, and ULTIMA III with Cu Kα radiation (λ = 1.5418 Å). Scanning electron microscope (SEM), VEGA-TESCAN, was utilized to identify surface morphology of the nanocomposites. Energy-dispersive X-ray spectroscopy (EDS) attached to SEM and this experiment was performed to recognize the chemical constituents of the samples. To determine the particle size and shape of the fillers, transmission electron microscope (TEM) was utilized using a JEOL JEM-2100 microscope. TEM study has been done in 200 KV. The scattering parameters corresponding to reflection (S_{11} or S_{22}) and transmission (S_{21} or S_{12}) were analyzed by utilizing vector network analyzer (PNA E8364B). Complex permittivity and permeability values were calculated from S_{11} and S_{21} values by means of materials measurement software (Agilent software module no. 85071) loaded in the vector network analyzer [19].

4. Results and Discussion

4.1. Structure and Morphology Analysis. XRD patterns of $Cu_{0.2}Ni_{0.4}Zn_{0.4}Fe_2O_4$ and $Pb(Zr_{0.52}Ti_{0.48})O_3$ nanoparticles are shown in Figure 1. The main peak of $Cu_{0.2}Ni_{0.4}Zn_{0.4}Fe_2O_4$ are at 2θ = 30.22°, 35.61°, 37.22°, 43.35°, 53.72°, 57.22°, 62.77°, 71.24°, 74.16°, and 75.18° revealing typical spinel structure [20]. The main peak of $Pb(Zr_{0.52}Ti_{0.48})O_3$ is at 2θ = 21.90°, 31.10°, 38.67°, 44.65°, 50.49°, 55.46°, 56.33° and 65.53° determining it is tetragonal perovskite structure (JCPDS PDF no. 01-070-4060) and the peaks at 2θ = 30.22°, 34.98°, and 60.06° originate due to ZrO_2 which is formed during the formation of PZT [21]. The other peaks of ZrO_2 are merged with the peaks of lead zirconium titanate.

Figure 2 shows the SEM images of fracture site of Sample-3 in secondary electron detector (SE detector) and back-scattered electron detector (BSE detector). SEM image in SE detector showed the dispersion of nanofillers in the polymeric matrix; different sized nanoparticles were well distributed into the polymeric matrix (Figure 2(a)). From the SEM image in BSE detector, the bright spots were nicely seen, which clearly demonstrate the dispersion of the heavy particles into the polymeric matrix (Figure 2(b)). Figure 3 represents the EDS of Sample-3 and this experiment was performed from region A in Figure 2(a). EDS analysis has been carried out to identify elemental composition of the prepared materials. The EDS attached to SEM confirmed the presence of chemical constituents, for example, oxygen (O), carbon (C), lead (Pb), zirconium (Zr), titanium (Ti), copper (Cu), nickel (Ni), zinc (Zn), and iron (Fe) (Figure 3). To ensure electrical conductivity of the polymer nanocomposites, a thin layer of gold was sputtered on fracture surface of the samples. Due to this, gold (Au) was present in the EDS spectrum.

Figure 4(a) shows the TEM image of Cu-NZF nanoparticles. Cubic-sized Cu-NZF nanoparticles were formed with different sizes. The maximum particle size of ferrite was ~100 nm. From TEM image of PZT (Figure 4(b)), it was seen that that the average particle sizes were ~35 nm and they were almost spherical. Figure 4(c) shows the TEM image of

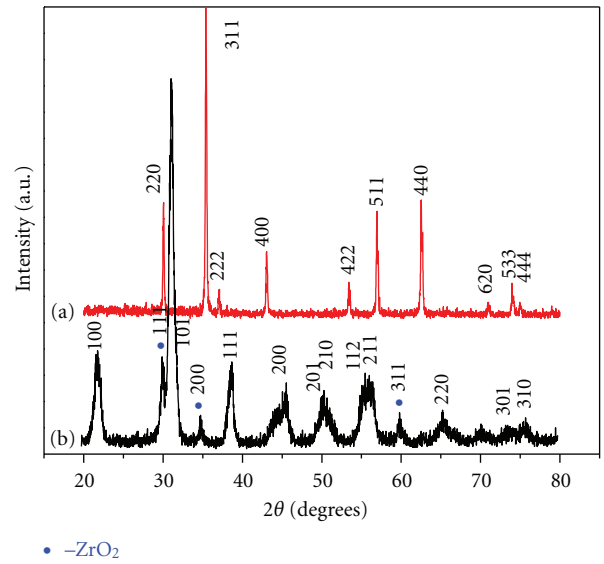

FIGURE 1: XRD patterns of (a) $Cu_{0.2}Ni_{0.4}Zn_{0.4}Fe_2O_4$ and (b) $Pb(Zr_{0.52}Ti_{0.48})O_3$ nanoparticles.

Sample-3, it shows that the cubic and spherical nanoparticles were closely associated with each other, which could be due to interaction between dielectric and magnetic dipoles.

4.2. Microwave Absorbing Properties. The microwave absorbing properties of the developed nanocomposites with different thicknesses in the X-band region are shown in Figures 5(a)–5(e). Samples-1, -2, and -3 showed minimum return loss of −29.85 dB at 8.79 GHz, −43.82 dB at 8.95 GHz, and −49.53 dB at 8.44 GHz, respectively, when thickness of the samples was 3 mm (Figures 5(a), 5(b), and 5(c)). Samples-4, -5 achieved minimum return loss of −46.36 dB at 9.04 GHz and −37.46 dB at 8.37 GHz when sample thickness was 2.75 and 3 mm, respectively, (Figures 5(d) and 5(e)).

From the above results, it was seen that with increasing thickness, the dip of return loss values shifted toward lower frequency region. The present nanocomposites achieved better microwave absorbing properties when thickness of the samples was 3 mm; that is, 3 mm thickness was the matching thickness for the present absorbers. All the nanocomposites showed excellent microwave absorbing properties and out of these five samples, Sample-3 showed better absorbing properties. The mechanism of absorption has been clearly resolved with the help of real and imaginary parts of permittivity, permeability values. In the present research work, the nanocomposites achieved better microwave absorbing properties compared to NiZn-NiCuZn ferrite/epoxy resin [22], Cu-doped Ni-Zn spinel ferrite/paraffin [20], ZnO/$CoFe_2O_4$ nanocomposites [23], and (Co^{2+}-Si^{4+}) substituted barium hexaferrite composite [24] systems.

4.3. Permittivity and Permeability Spectra. Real and imaginary parts of permittivity and permeability are the most important parameters to elucidate the possible mechanisms

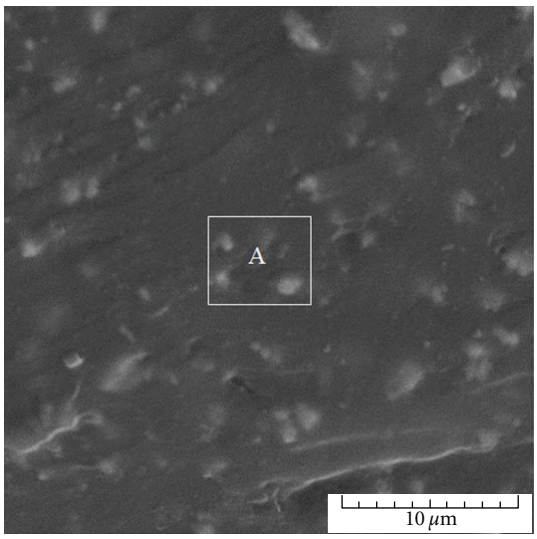

(a)

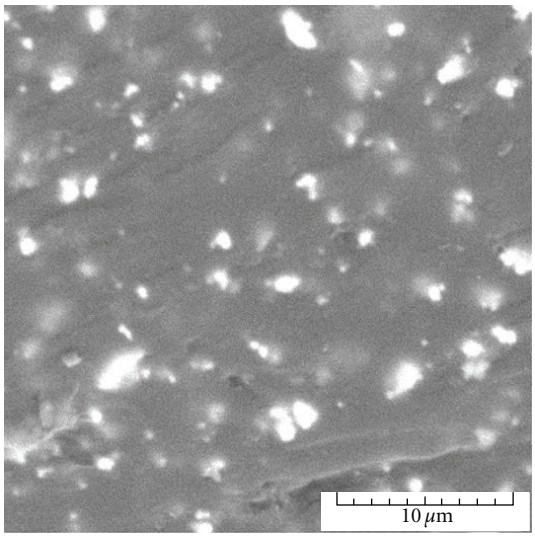

(b)

Figure 2: SEM images of Sample-3 (a) in secondary electron detector (SE detector) and (b) in back scattered electron detector (BSE detector).

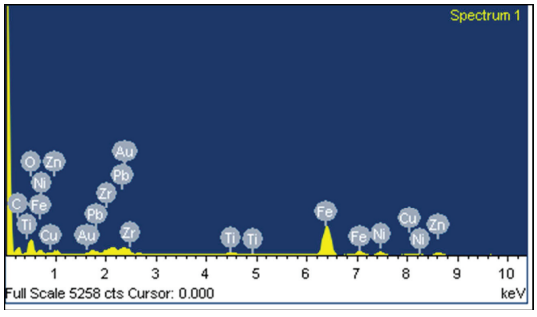

Figure 3: EDS analysis of Sample-3.

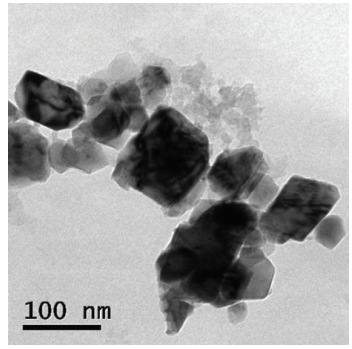

(a)

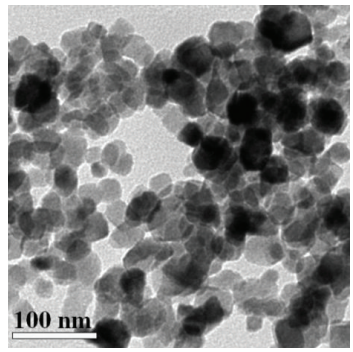

(b)

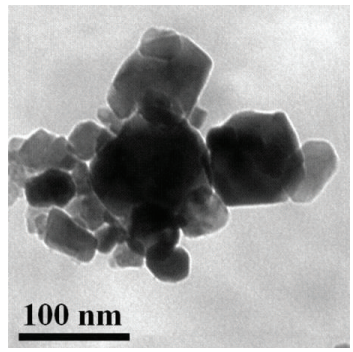

(c)

Figure 4: TEM images of (a) $Cu_{0.2}Ni_{0.4}Zn_{0.4}Fe_2O_4$ (Cu-NZF) nanoparticles, (b) $Pb(Zr_{0.52}Ti_{0.48})$ O_3(PZT) nanoparticle, and (c) Sample-3.

of microwave power absorption. Figures 6(a) and 6(b) show the real (ε') and imaginary (ε'') parts of permittivity and Figures 6(c) and 6(d) show the real (μ') and imaginary (μ'') parts of permeability, respectively. The ε' and μ' values stand for electric and magnetic energy storage parts while ε'' and μ'' values stand for electric and magnetic energy loss parts. The storages of electric and magnetic energy are caused by polarizations of electrical and magnetic dipoles. Dielectric and magnetic losses are caused by relaxation phenomena of dipoles resulting dissipation of microwave energy as heat. The real parts (ε') of permittivity of Sample-1, -2, -3, -4, and -5 were approximately 3.8, 3.9, 4, 4.16, and 4.5 respectively. The

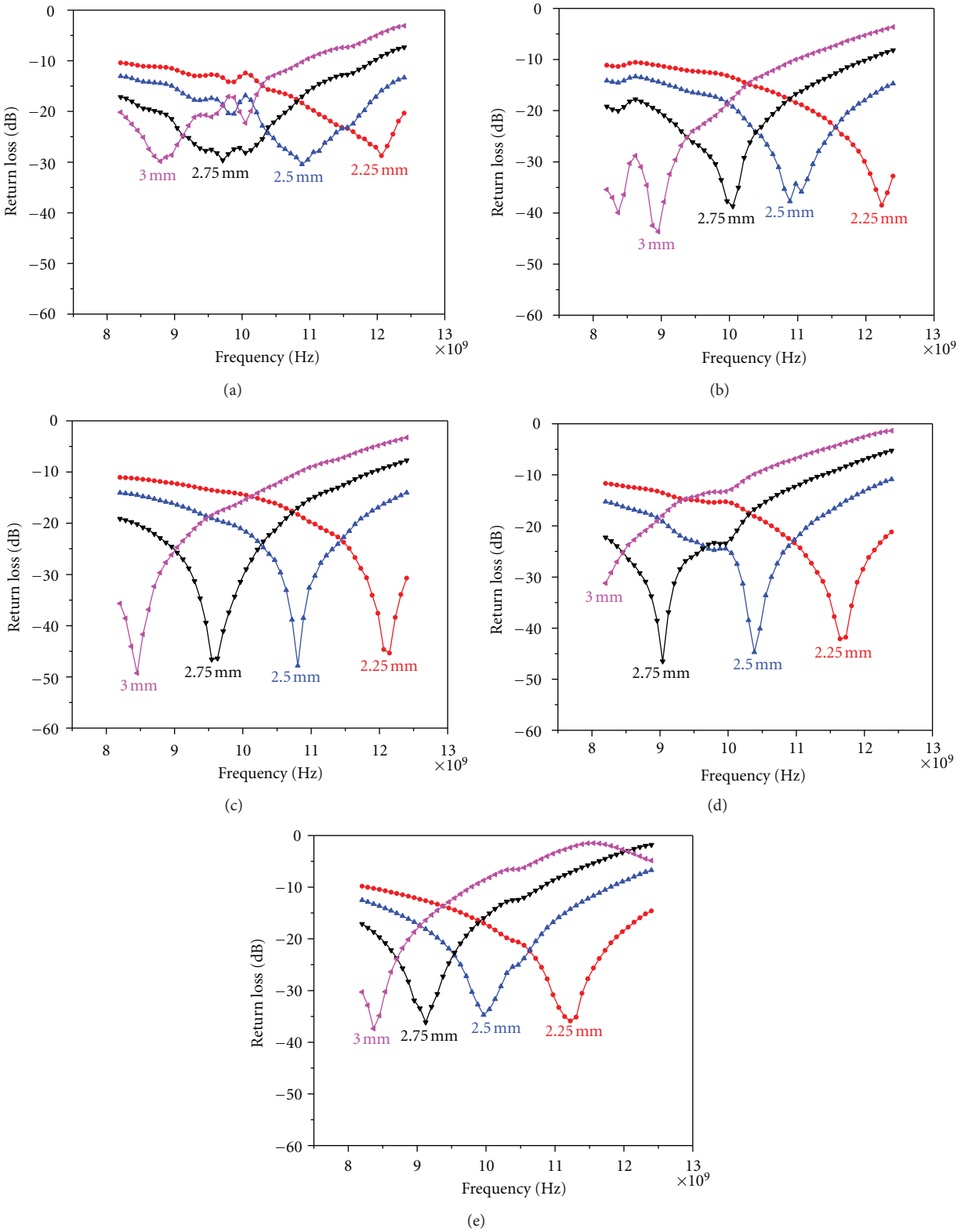

FIGURE 5: Microwave absorbing properties of (a) Sample-1, (b) Sample-2, (c) Sample-3, (d) Sample-4, and (e) Sample-5 with different thicknesses.

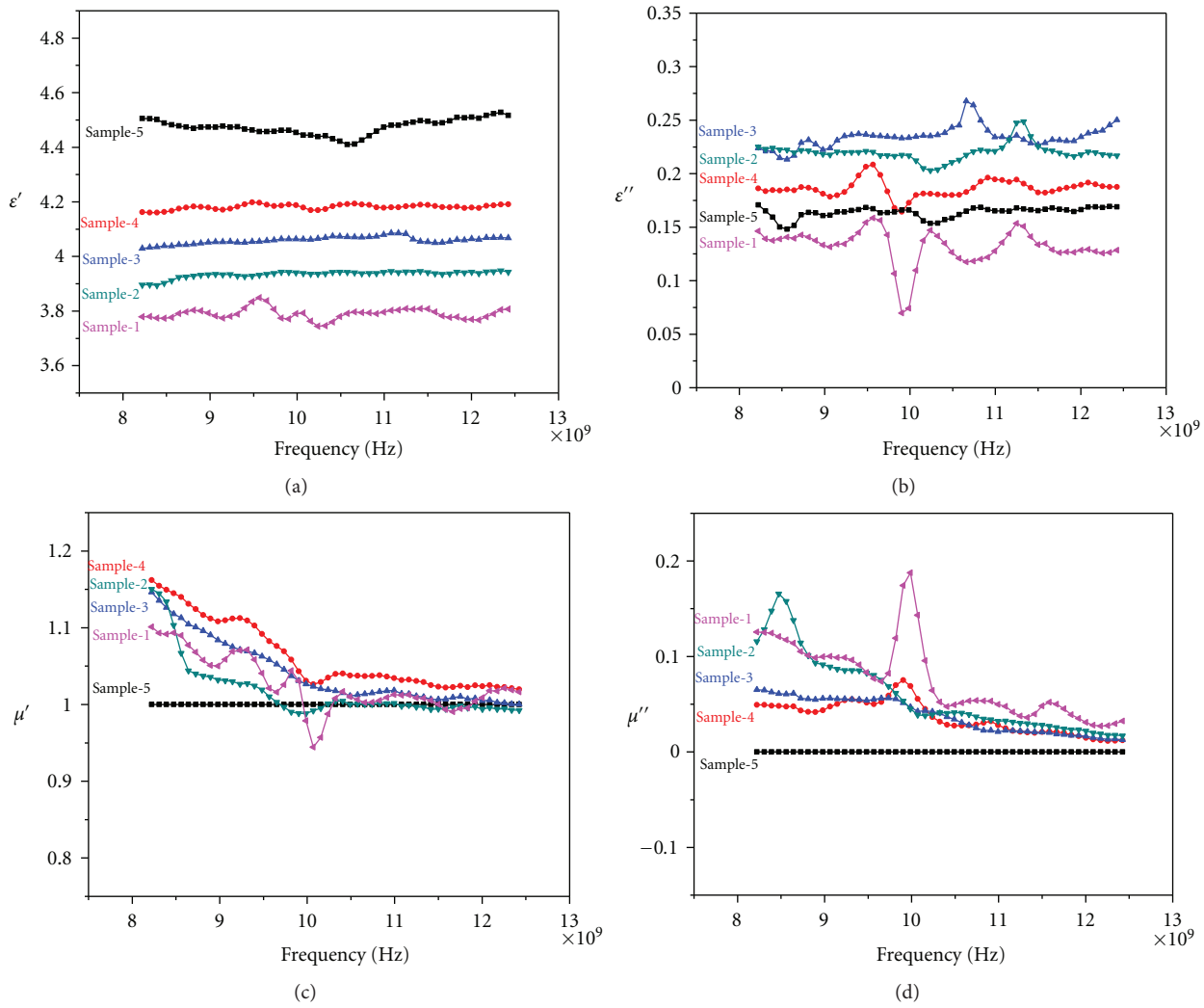

FIGURE 6: (a) Real (ε') and (b) imaginary (ε'') parts of relative complex permittivity; (c) real (μ') and (d) imaginary (μ'') parts of relative complex permeability of prepared samples.

imaginary parts of permittivity (ε''), that is, dielectric loss for Sample-1, lied from 0.15 to 0.13 with a main resonance peak at 9.58 GHz. The ε'' value for Sample-2 lied from 0.225 to 0.22. The ε'' value changed from 0.224 to 0.25 for Sample-3. Samples-4 and -5 showed the dielectric loss values ~ 0.19 and ~0.17, respectively. The real parts of permeability (μ') values of Samples-1 to -4 at relatively higher frequency (10–12.4 GHz) were close to 1. The μ' value for Sample-4 was the highest and ranging from 1.16 to 1.01. The μ'' value of Sample-1 was the highest and ranging from 0.13 to 0.03 with a main resonance peak at 9.98 GHz. As the Sample-5 was purely dielectric, the μ' and μ'' values of Sample-5 were 1 and 0, respectively.

Lead zirconium titanate has permanent electric dipoles. Since the nanocomposites were heterogeneous systems, interfacial polarization happened at the interfaces between nanofillers and polymeric matrices. The real part of permittivity (ε'), that is, dielectric constant, is directly depending on electric polarizations. Due to this the ε' values were increased with increasing the concentration of PZT (from Sample-1 to -5). The ε'' values of the nanocomposites showed a decreasing trend with frequency and were not so linear with frequency due to relaxation phenomena of dipoles. The nanocomposites achieved excellent absorbing properties when both ferromagnetic and ferroelectric materials were present. From Figure 6(b), it can be concluded that absorbing performance of the present nanocomposites was directly depending on the dielectric loss part except Sample-4. Sample-3 exhibited the better absorbing properties due to high dielectric loss than other absorbers. In case of Sample-3, the permanent polarizations, dominant polarizations, and their corresponding relaxation phenomena should be high [23]. Sample-2 showed higher dielectric loss values than Sample-4 but Sample-4 achieved better properties than Sample-2 due to the relatively higher

value of μ'. From Figure 6(c), it was seen that the real part of permeability (μ') values of the absorbers showed a decreasing trend with increasing frequency. At higher frequency the external field changes rapidly, so that the realignment of magnetic dipoles with external field is too difficult. For this reason the real part of permeability (μ') decreases with increasing frequency and imaginary parts of permeability (μ'') also decreased with increasing frequency. The magnetic loss depends on saturation magnetization and coercivity of magnetic material. Due to the Cu-substitution in nickel zinc ferrite, the saturation magnetization is increased and coercivity is decreased [22]. Magnetic field loss is caused by eddy current loss and residual loss [25]. The magnetic losses of the samples have small values and close to each other. Permanent polarization, dominant polarization, and the associated relaxation phenomena are responsible for loss mechanism.

5. Conclusions

Development of nanocomposites based on $Cu_{0.2}Ni_{0.4}Zn_{0.4}Fe_2O_4$ and $Pb(Zr_{0.52}Ti_{0.48})O_3$ has been confirmed successfully by XRD, EDS, and TEM analyses. Complex permittivity and permeability values established prominently the possible mechanism of absorption; that is, the relation between permittivity and permeability with the microwave power absorbing performance was elucidated precisely. All the developed materials achieved attractive microwave absorbing properties in the X-band region. Sample-3 exhibited the minimum return loss of −49.53 dB at 8.44 GHz when sample thickness was 3 mm. Thus, out of these five samples, Sample-3 was the optimal microwave absorbing material. Impedance matching and thickness matching effects are the most important parameters to investigate attractive microwave absorbing materials.

Acknowledgments

The authors are grateful for the financial support from the Council of Scientific and Industrial Research (CSIR), New Delhi, and also special thanks to director, DMSRDE, Kanpur for providing the facility of microwave absorbing measurements.

References

[1] Y. B. Feng, T. Qiu, C. Y. Shen, and X. Y. Li, "Electromagnetic and absorption properties of carbonyl iron/rubber radar absorbing materials," *IEEE Transactions on Magnetics*, vol. 42, no. 3, pp. 363–368, 2006.

[2] P. B. Jana, A. K. Mallick, and S. K. De, "Effects of sample thickness and fiber aspect ratio on EMI shielding effectiveness of carbon fiber filled polychloroprene composites in the X-band frequency range," *IEEE Transactions on Electromagnetic Compatibility*, vol. 34, no. 4, pp. 478–481, 1992.

[3] M. A. Soloman, P. Kurian, M. R. Anantharaman, and P. A. Joy, "Evaluation of the magnetic and mechanical properties of rubber ferrite composites containing strontium ferrite," *Polymer - Plastics Technology and Engineering*, vol. 43, no. 4, pp. 1013–1028, 2004.

[4] S. M. Abbas, M. Chandra, A. Verma, R. Chatterjee, and T. C. Goel, "Complex permittivity and microwave absorption properties of a composite dielectric absorber," *Composites Part A*, vol. 37, no. 11, pp. 2148–2154, 2006.

[5] J. Y. Shin and J. H. Oh, "Microwave absorbing phenomena of ferrite microwave absorbers," *IEEE Transactions on Magnetics*, vol. 29, no. 6, pp. 3437–3439, 1993.

[6] M. Pardavi-Horvath, "Microwave applications of soft ferrites," *Journal of Magnetism and Magnetic Materials*, vol. 215-216, pp. 171–183, 2000.

[7] C. H. Peng, C. C. Hwang, J. Wan, J. S. Tsai, and S. Y. Chen, "Microwave-absorbing characteristics for the composites of thermal-plastic polyurethane (TPU)-bonded NiZn-ferrites prepared by combustion synthesis method," *Materials Science and Engineering B*, vol. 117, no. 1, pp. 27–36, 2005.

[8] F. M. M. Pereira, M. R. P. Santos, R. S. T. M. Sohn et al., "Magnetic and dielectric properties of the M-type barium strontium hexaferrite ($Ba_xSr_{1-x}Fe_{12}O_{19}$) in the RF and microwave (MW) frequency range," *Journal of Materials Science*, vol. 20, no. 5, pp. 408–417, 2009.

[9] H. M. Xiao, X. M. Liu, and S. Y. Fu, "Synthesis, magnetic and microwave absorbing properties of core-shell structured $MnFe_2O_4/TiO_2$ nanocomposites," *Composites Science and Technology*, vol. 66, no. 13, pp. 2003–2008, 2006.

[10] J. Qiu, L. Lan, H. Zhang, and M. Gu, "Microwave absorption properties of nanocomposite films of $BaFe_{12}O_{19}$ and TiO_2 prepared by sol-gel method," *Materials Science and Engineering B*, vol. 133, no. 1–3, pp. 191–194, 2006.

[11] P. Singh, V. K. Babbar, A. Razdan, R. K. Puri, and T. C. Goel, "Complex permittivity, permeability, and X-band microwave absorption of CaCoTi ferrite composites," *Journal of Applied Physics*, vol. 87, no. 9, pp. 4362–4366, 2000.

[12] A. Verma, A. K. Saxena, and D. C. Dube, "Microwave permittivity and permeability of ferrite-polymer thick films," *Journal of Magnetism and Magnetic Materials*, vol. 263, no. 1-2, pp. 228–234, 2003.

[13] S. B. Cho, D. H. Kang, and J. H. Oh, "Relationship between magnetic properties and microwave-absorbing characteristics of NiZnCo ferrite composites," *Journal of Materials Science*, vol. 31, no. 17, pp. 4719–4722, 1996.

[14] P. Singh, V. K. Babbar, A. Razdan, S. L. Srivastava, and T. C. Goel, "Microwave absorption studies of Ca-NiTi hexaferrite composites in X-band," *Materials Science and Engineering B*, vol. 78, no. 2-3, pp. 70–74, 2000.

[15] S. S. Kim, S. B. Jo, K. I. Gueon, K. K. Choi, J. M. Kim, and K. S. Churn, "Complex permeability and permittivity and microwave absorption of ferrite-rubber composite at X-band frequencies," *IEEE Transactions on Magnetics*, vol. 27, no. 6, pp. 5462–5464, 1991.

[16] T. Nakamura, "Snoek's limit in high-frequency permeability of polycrystalline Ni-Zn, Mg-Zn, and Ni-Zn-Cu spinel ferrites," *Journal of Applied Physics*, vol. 88, no. 1, pp. 348–353, 2000.

[17] H. Y. He, "Magnetic properties of $Co_{0.5}Zn_{0.5}Fe_2O_4$ nanoparticles synthesized by a template-assisted hydrothermal method," *Journal of Nanotechnology*, vol. 2011, Article ID 182543, 5 pages, 2011.

[18] A. C. Taş, "Preparation of lead zirconate titanate ($Pb(Zr_{0.52}Ti_{0.48})O_3$) by homogeneous precipitation and calcination," *Journal of the American Ceramic Society*, vol. 82, no. 6, pp. 1582–1584, 1999.

[19] Hewlett-Packard microwave network analyzer catalog no. 8510 and product note no. 8510-3, 1987.

[20] F. Gao, D. L. Zhao, and Z. M. Shen, "Preparation and microwave absorbing properties of Cu-doped Ni-Zn spinel ferrites," *Advanced Materials Research*, vol. 105-106, no. 1, pp. 293–296, 2010.

[21] G. Duan, C. Zhang, A. Li, X. Yang, L. Lu, and X. Wang, "Preparation and characterization of mesoporous zirconia made by using a poly (methyl methacrylate) template," *Nanoscale Research Letters*, vol. 3, no. 3, pp. 118–122, 2008.

[22] J. C. Aphesteguy, A. Damiani, D. DiGiovanni, and S. E. Jacobo, "Microwave-absorbing characteristics of epoxy resin composites containing nanoparticles of NiZn- and NiCuZn-ferrites," *Physica B*, vol. 404, no. 18, pp. 2713–2716, 2009.

[23] J. Cao, W. Fu, H. Yang et al., "Large-scale synthesis and microwave absorption enhancement of actinomorphic tubular $ZnO/CoFe_2O_4$ nanocomposites," *Journal of Physical Chemistry B*, vol. 113, no. 14, pp. 4642–4647, 2009.

[24] S. M. Abbas, R. Chatterjee, A. K. Dixit, A. V. R. Kumar, and T. C. Goel, "Electromagnetic and microwave absorption properties of (Co^{2+}-Si^{4+}) substituted barium hexaferrites and its polymer composite," *Journal of Applied Physics*, vol. 101, no. 7, Article ID 074105, 2007.

[25] P. J. Van Der Zaag, "New views on the dissipation in soft magnetic ferrites," *Journal of Magnetism and Magnetic Materials*, vol. 196-197, pp. 315–319, 1999.